Monthly Notices of the ROYAL ASTRONOMICAL SOCIETY

Mon. Not. R. Astron. Soc. **409,** 1518–1524 (2010) doi:10.1111/j.1365-2966.2010.17379.x

Quantifying the importance of ram-pressure stripping in a galaxy group at 100 Mpc

E. Freeland,[1★] C. Sengupta[2,3★] and J. H. Croston[4★]

[1] *George P. & Cynthia W. Mitchell Institute for Fundamental Physics and Astronomy, Department of Physics and Astronomy, Texas A&M University, College Station, TX 77843, USA*
[2] *Calar-Alto Observatory, Centro Astronomico Hispano Aleman, C/Jesus Durban Remon, 2-2 04004 Almeria, Spain*
[3] *Instituto de Astrofisica de Andalucia (CSIC), Glorieta de Astronomia s/n, 18008 Granada, Spain*
[4] *School of Physics and Astronomy, University of Southampton, Southampton SO17 1SJ*

Accepted 2010 July 17. Received 2010 July 12; in original form 2010 May 14

ABSTRACT

We examine two members of the NGC 4065 group of galaxies: a bent-double (aka wide angle tail) radio source and an H I-deficient spiral galaxy. Models of the X-ray-emitting intragroup gas and the bent-double radio source, NGC 4061, are used to probe the density of intergalactic gas in this group. H I observations reveal an asymmetric, truncated distribution of H I in spiral galaxy, UGC 07049, and the accompanying radio continuum emission reveals strong star formation. We examine the effectiveness of ram-pressure stripping as a gas-removal mechanism and find that it alone cannot account for the H I deficiency that is observed in UGC 07049 unless this galaxy has passed through the core of the group with a velocity of $\sim 800\,\mathrm{km\,s^{-1}}$. A combination of tidal and ram-pressure stripping are necessary to produce the H I deficiency and asymmetry in this galaxy.

Key words: galaxies: evolution – galaxies: groups: individual: NGC 4065 – intergalactic medium – galaxies: jets.

1 INTRODUCTION

Galaxy characteristics, like morphology and star formation rate (SFR), are observed to change with environment where high-density regions like clusters are characterized by a larger fraction of elliptical galaxies and a lower star formation rate than seen in the field (Dressler 1980; Gómez et al. 2003; Goto et al. 2003). These observations are known as the morphology–density and SFR–density relations, although Whitmore et al. (1991, 1993) argue that these reflect a tighter and more fundamental morphology–radius relation where the distance from the cluster centre is the independent parameter. The morphology–density relation shows distinct behaviour over three separate regimes which can be characterized in terms of the projected galaxy density or the radial distance from the cluster centre [in terms of the virial radius, R_{vir}, defined by Girardi et al. (1998) as $R_{\mathrm{vir}} \simeq 0.002\sigma_r\ h_{100}^{-1}\,\mathrm{Mpc}$]. In the lowest density regions farthest from cluster centres (with projected densities of $<1\,\mathrm{Mpc^{-2}}$ or radius of $>1R_{\mathrm{vir}}$) the relation is flat, suggesting that the physical mechanisms responsible for changes in morphology are not effective in this regime. At a characteristic radius of $\sim 1R_{\mathrm{vir}}$ (projected densities of 1–6 $\mathrm{Mpc^{-2}}$) the fraction of intermediate-type (S0) galaxies begins to increase while the late-type disc (Sc) galaxy fraction decreases and the SFR decreases sharply (Gómez et al. 2003). These trends continue till $\sim 0.3R_{\mathrm{vir}}$ (projected density of $>6\,\mathrm{Mpc^{-2}}$) where the fraction of intermediate types decreases and the elliptical fraction dramatically increases (Goto et al. 2003). The behaviour of these relations over the separate regimes indicates a change in the dominant physical mechanisms influencing the evolution of galaxies across these environments.

There are a variety of physical mechanisms that could be responsible for altering galaxy morphology in dense environments, including ram-pressure stripping, tidal interactions, galaxy harassment, strangulation and major and minor mergers. The vast majority of galaxies reside in groups which are small dynamical systems typically containing a handful of large ($\sim L_*$) galaxies and a large number of smaller galaxies (Geller & Huchra 1983; Tully 1987; Eke 2004; Yang et al. 2007; Tago et al. 2008). These systems have velocity dispersions between ∼30 and 500 $\mathrm{km\,s^{-1}}$ and intragroup medium (IGM) densities that are not well constrained. Thus, it has been thought that tidal interactions are likely to dominate in this environment while ram-pressure stripping and strangulation are less likely to be important.

Galaxy groups, according to the hierarchical scenario of the formation of large-scale structure, are the building blocks of rich clusters of galaxies. Since most galaxies exist in groups these are important sites in which to investigate the physical mechanisms responsible for the observed morphology and SFR–density relations. Two important questions arise.

★E-mail: freeland@physics.tamu.edu (EF); chandra@caha.es (CS); J.Croston@soton.ac.uk (JHC)

(i) To what extent are field galaxies and intergalactic gas pre-processed by the group environment before they are incorporated into galaxy clusters?

(ii) Which physical mechanisms are important in altering the morphology and SFR of galaxies in the group environment?

Here we present observations of the NGC 4065 group, located in the Coma supercluster. This group is a unique laboratory for studying ram-pressure stripping as we have two independent means of measuring the density of the intergalactic gas in this system which also contains an H I-deficient, edge-on, Sc galaxy (UGC 07049). This group has an average velocity of 6995 ± 48 km s^{-1}($z = 0.0233$), a velocity dispersion of 416 ± 35 km s^{-1} and extended X-ray emission from the IGM (Mahdavi & Geller 2004). Our Very Large Array (VLA) D-array data show numerous interactions among H I-rich group members outside of the core of the group (Freeland, Stilp & Wilcots 2009). Gavazzi et al. (2006) classify UGC 07049 as strongly H I deficient using Arecibo data and find that it has a total H I mass of 2×10^9 M$_\odot$. This group is also known as RASSCALS NRGb 177 (Mahdavi et al. 2000), GEMS NGC 4065 (Osmond & Ponman 2004) and GH 98 (Geller & Huchra 1983).

At the distance of this group 1 arcmin corresponds to ∼30 kpc. We use a Hubble constant of 75 km s^{-1} Mpc^{-1}.

2 OBSERVATIONS

2.1 GMRT data

The NGC 4065 group was observed with the Giant Metrewave Radio Telescope (GMRT) at 610 MHz in the standard continuum observing mode in 2007 August for 8 h including calibration. Both the upper and lower sidebands of the correlator were used with 16-MHz bandwidth in each. Here we present only upper sideband data.

The group was observed in H I 21-cm line using the GMRT in 2008 May. At 1420 MHz, the system temperature and the gain (K/Jy) of the instrument are 76 K and 0.22, respectively. The observations were carried out in the Indian polar mode. The baseband bandwidth used was 16 MHz, giving a velocity resolution of 27 km s^{-1}. The on-source integration time was 15 h. The pointing centre for the H I observations was $12^{\rm h}04^{\rm m}01\overset{\rm s}{.}5 + 20^\circ 13' 54\overset{''}{.}34$ in J2000 coordinates.

The radio data were reduced using Astronomical Image Processing System (AIPS) using standard procedures. Bad data due to dead antennas and radio frequency interference (RFI) were flagged and the data were calibrated for amplitude and phase using the primary and secondary calibrators. The primary calibrator was also used as the bandpass calibrator. The 20-cm radio continuum maps were made using the self-calibrated line-free channels of the observations. The radio continuum was then subtracted from the data using the AIPS tasks UVSUB and UVLIN. The final three-dimensional deconvolved H I data cubes were then obtained from the continuum subtracted data using the task IMAGR. From these cubes the total H I images and the H I velocity fields were extracted using the task MOMNT.

2.2 *XMM–Newton* data

A short archival *XMM–Newton* observation of the environment of radio source NGC 4061 (observation ID 0112271101, carried out on 2003 June 30) was used to study the X-ray emission from the IGM. The X-ray data were reprocessed using the *XMM–Newton* SAS version 6.0.0, and the latest calibration files from the *XMM–Newton* web site. The pn data were filtered to include only single and double events (PATTERN ≤ 4), and FLAG == 0, and the MOS data were filtered according to the standard flag and pattern masks (PATTERN ≤ 12 and #XMMEA_EM, excluding bad columns and rows). The data set was affected by background flares, so filtering for good time intervals was applied to ensure that accurate measurements could be made in low surface brightness regions. Light curves in the 10–12 keV (MOS) or 12–14 keV (pn) energy bands were used to identify time periods of high background rate, and thresholds of 0.4 count s^{-1} (MOS) and 0.7 count s^{-1} (pn) were applied. The exposure times remaining after good time interval (GTI) filtering were 5677, 6032 and 3335 s for the MOS1, MOS2 and pn cameras, respectively.

Spectral and spatial analysis were carried out using the filtered *XMM–Newton* events lists. The background was accounted for accurately using the double subtraction method described in Croston et al. (2008), which makes use of filter-wheel-closed data sets to constrain the instrumental and particle components of the background. Both source and background (filter-wheel-closed) events lists were vignetting corrected using the SAS task evigweight. The background data sets were scaled to account for differences in the level of the instrumental and particle background components using a weighting factor consisting of the ratio of source to background 10–12 keV count rate in a large background annulus. For surface brightness profile analysis, a background profile was first obtained by extracting a profile matched to the source profile from the weighted background file. The difference in background level between source and background profiles in the outer regions (where source emission should be negligible) was used as a second background component to subtract off the soft X-ray background from Galactic and cosmic X-ray components. For spectral analysis an equivalent process was used: spectra were obtained from the source and appropriate background events lists for both target and local background extraction regions. The Galactic/cosmic X-ray background contribution was modelled by fitting an X-ray background model to the local background spectrum consisting of two mekal models to account for emission from the Galactic bubble and a power-law model absorbed by the Galactic $N_{\rm H}$ in the direction of the target to account for the cosmic X-ray background. The mekal temperatures were allowed to vary, but the power-law index was fixed at $\Gamma = 1.41$ (Lumb et al. 2002). The normalizations of all three components were allowed to vary. For each source spectrum, we used the corresponding filter-wheel-closed spectrum as a background spectrum, to account for particle background, and a fixed X-ray background model consisting of the best-fitting model from the fit to the outer, source-free region, with the normalizations of each component fixed at the best-fitting values scaled to the appropriate area for the source-extraction region.

We extracted spectra for the group emission from an annular region of an inner radius of 2 arcmin (to exclude any active galactic nucleus related X-ray emission) and an outer radius of 6.7 arcmin. The spectra were fitted with a mekal model in additional to the fixed X-ray background model as described above. The best-fitting model parameters for a joint fit to the MOS1 and pn spectra in the energy range 0.3–7.0 keV were $kT = 1.31^{+0.14}_{-0.23}$ keV and $Z = 0.33^{+0.28}_{-0.19}$ Z$_\odot$ using a Galactic $N_{\rm H} = 2.3 \times 10^{20}$ cm^{-2}, giving $\chi^2 = 234$ for 186 d.o.f.

Surface brightness profiles were extracted from the MOS1 and pn events lists, which showed evidence for both an inner galaxy-scale halo and a flatter, group-scale component. A single β-model fit to the profiles was therefore a poor fit. We fitted the profiles with the projected double-β model as described in Croston et al.

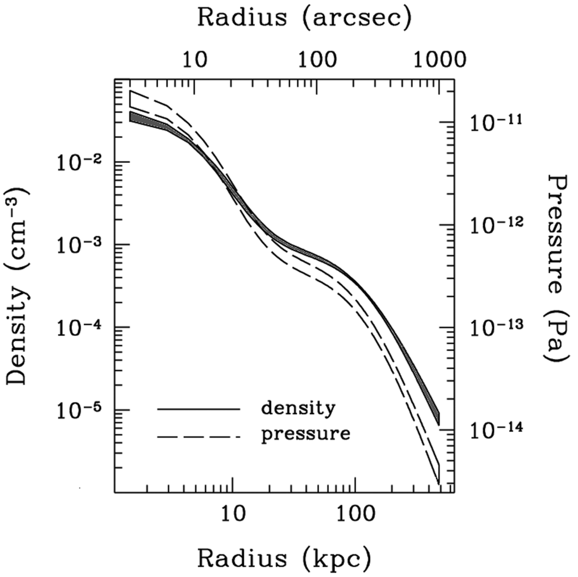

Figure 1. Number density and pressure profiles from the model fits to the *XMM–Newton* data showing the X-ray-emitting gas in this group. The pressure profile is calculated from the density profile assuming temperature, $kT = 1.31$ keV. Uncertainties (1σ) in the density and pressure are illustrated by the width of the curves.

(2008), which is the surface brightness profile corresponding to a gas density profile of

$$n(r) = n_0 \left[\left(1 + \frac{r^2}{r^2_{c,\mathrm{in}}}\right)^{-3\beta_{\mathrm{in}}/2} + N \left(1 + \frac{r^2}{r^2_c}\right)^{-3\beta/2} \right], \qquad (1)$$

where N is the relative normalization of the two-β model component. Before fitting, each model was convolved with the *XMM–Newton* point spread function (PSF) based on the on-axis parametrization described in the *XMM–Newton* Current Calibration Files (CCF) XRT1_XPSF_0006.CCF, XRT2_XPSF_0007.CCF and XRT3_XPSF_0007.CCF. The Markov chain Monte Carlo (MCMC) method for exploring the six-dimensional parameter space for this model described in Croston et al. (2008) was used to determined the best-fitting model parameters for the gas density profile, with the joint χ^2 value for the three profiles as the likelihood estimator. Plausible ranges for each parameter were estimated by carrying out extreme fits and these were used as priors for the MCMC method. Quantities derived from the surface brightness model fits, including X-ray luminosity and pressure at a given radius, are obtained by determining that quantity for each model fit and then obtaining the Bayesian estimate for the quantity in question. Uncertainties on the derived quantities are the minimal one-dimensional interval enclosing 68 per cent of the values for the given quantity, and so correspond to the 1σ intervals for one interesting parameter. Some of the parameters are strongly correlated, leading to large uncertainties on the individual model parameters; however, tight constraints can be obtained on derived quantities such as pressure and luminosity. The best-fitting model parameters were $\beta_{\mathrm{in}} = 1.2$, $r_{c,\mathrm{in}} = 13.1$ arcsec, $\beta = 1.2$, $r_c = 256$ arcsec and $N = 0.024\,53$ with $\chi^2 = 24.4$ for 16 d.o.f. Fig. 1 shows the number density profile for the hot intergalactic gas in the core of this group.

3 GROUP DYNAMICS

We rely on the redshift survey of this group performed by Mahdavi & Geller (2004) which finds 74 members with an average velocity of $6995 \pm 48\,\mathrm{km\,s^{-1}}$ and a velocity dispersion of $416 \pm 35\,\mathrm{km\,s^{-1}}$ (see Fig. 2). The group has two compact subgroups, UZG-CG 156 (including NGC 4076) and UZC-CG 157 (including NGC 4061), which were identified by the three-dimensional Updated Zwicky Catalogue (Falco et al. 1999) solely on the criterion of compactness (Focardi & Kelm 2002). These two subgroups are not distinguishable by velocity. However, there does appear to be an extended tail in the distribution towards lower velocities. The galaxies in this extended tail are clustered on the sky near UZC-CG 156 and may represent a filament towards nearby (~6° away) rich cluster Abell 1367 whose velocity is $6595\,\mathrm{km\,s^{-1}}$.

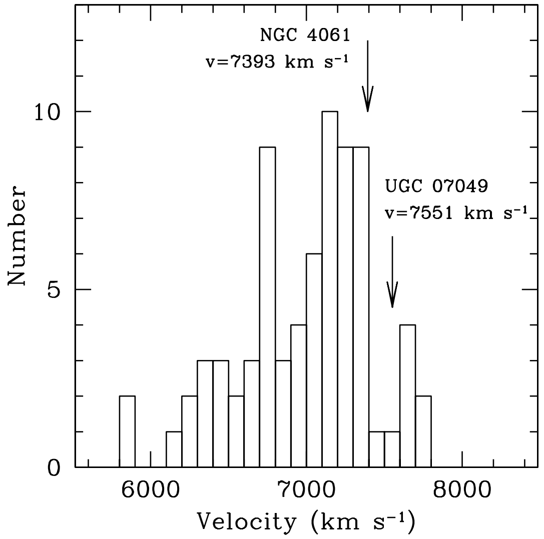

Figure 2. Histogram of velocities for the NGC 4065 group of galaxies from the data in Mahdavi & Geller (2004). The velocity of bent-double radio source NGC 4061 and that of spiral galaxy UGC 07049 are indicated with arrows. The bins are $100\,\mathrm{km\,s^{-1}}$ wide.

If we assume that the extended tail is not significantly dynamically associated with the NGC 4065 group, and we remove those velocities from the sample, then the velocity dispersion becomes $220 \pm 30\,\mathrm{km\,s^{-1}}$. The errors on this velocity dispersion are determined by generating bootstrap samples.

The lack of simple Gaussianity in the distribution of velocities and the strong spatial bimodality in the diffuse X-ray emission indicates that the system is not in dynamical equilibrium. If we assume the that group potential is deepest at the peak of the velocity histogram, then the X-ray gas of this peak is located at a velocity of $\sim 7150\,\mathrm{km\,s^{-1}}$. The velocity of NGC 4065 ($v = 6326\,\mathrm{km\,s^{-1}}$), the early-type galaxy immediately east of radio galaxy NGC 4061, puts it likely outside of the core of the group despite its projected appearance. The velocity of bent-double radio galaxy, NGC 4061, as measured by Mahdavi & Geller (2004) is $7393 \pm 32\,\mathrm{km\,s^{-1}}$. Previous radial velocity measurements have given this source a velocity of $7203 \pm 27\,\mathrm{km\,s^{-1}}$ (de Vaucouleurs et al. 1991) and $7369 \pm 52\,\mathrm{km\,s^{-1}}$ (Falco et al. 1999).

4 BENT-DOUBLE RADIO SOURCE NGC 4061

We follow the method for using bent-double radio sources as probes of intergalactic gas outlined in Freeland, Cardoso & Wilcots (2008) with a few additional caveats. We are assuming that the jet bulk flows have decelerated to non-relativistic speeds on kiloparsec scales, and certainly by the time they are bent by the motion of the host galaxy (~15 kpc from the core of the radio galaxy). This assumption is

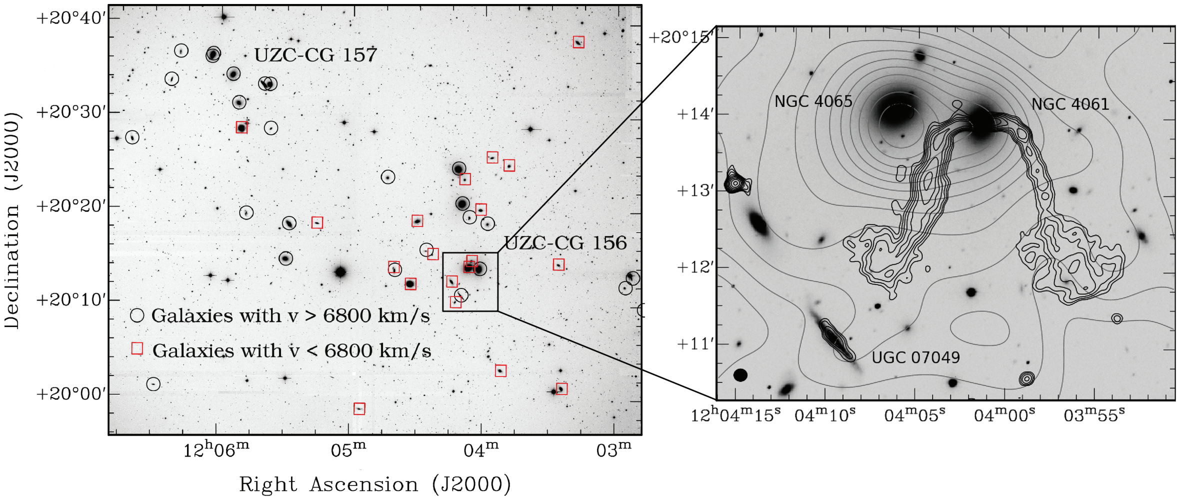

Figure 3. Left-hand panel: the spatial locations of galaxies with recessional velocities greater than 6800 km s^{-1} are marked with black circles. The spatial locations of galaxies with recessional velocities less than 6800 km s^{-1} are marked with red squares. The underlying image was taken in the optical *R* band. There are approximately 20 more galaxies identified as group members by Mahdavi & Geller (2004) which are beyond the edge of the optical image, mainly to the north and west. Right-hand panel: *XMM* X-ray (grey) and GMRT 60-cm radio continuum (black) contours overlaid on an optical *R*-band image of the core of the NGC 4065 galaxy group, also the core of compact subgroup UZC-CG 156. Radio continuum emission from the disc of spiral galaxy UGC 07049 indicates it has a high star formation rate. The 60-cm radio contours start at 1.4 mJy beam^{-1} and increase by $\sqrt{2}$. The 7.8 × 6.7 arcsec^2 60-cm beam is shown in the lower left-hand corner. At the distance of this group 1 arcmin corresponds to 30 kpc.

borne out by the symmetric fluxes in the two jets (see Fig. 3); were they still relativistic then beaming effects would produce asymmetric fluxes which would be easily observable in these data. We also consider additional pressure in the jets from entrained material.

Bent-double radio sources can be used to measure the density of intergalactic gas by the application of Euler's equation (Begelman, Rees & Blandford 1979; Jones & Owen 1979; Burns & Owen 1980). The time-independent Euler equation describes the balance of internal and external pressure gradients,

$$\frac{\rho_{\rm IGM} v_{\rm gal}^2}{h} = \frac{\rho_{\rm j} v_{\rm j}^2}{R}, \qquad (2)$$

where $\rho_{\rm IGM} v_{\rm gal}^2$ is the external ram pressure felt by the radio galaxy as it travels through the IGM, $\rho_{\rm j} v_{\rm j}^2$ is the internal pressure of the jet, h is the width of the jet and R is the radius of curvature of the jet. We estimate the speed of the radio galaxy using the group velocity dispersion. The pressure in the jets is determined at a position in the jet immediately before it bends using the minimum synchrotron pressure as outlined in O'Dea & Owen (1987). Standard equipartition of energy between relativistic particles and magnetic fields is assumed. We assume a radio spectral index of $\alpha = 0.55$ in the jets through the point where they bend as is seen in other Fanaroff–Riley type I (FR I) sources with high-resolution, multifrequency radio data (Young et al. 2005; Laing et al. 2008). Our values for the minimum synchrotron pressure in the jets are in good agreement with other measurements for similar radio sources (Venkatesan et al. 1994; Worrall & Birkinshaw 2000).

Observations of straight FR I sources show that the minimum synchrotron pressure in the jets does not balance the observed external pressure from the intergalactic gas as measured by modelling its X-ray emission (Bicknell 1984; Laing & Bridle 2002; Croston et al. 2008). The standard assumption is that entrained thermal protons are likely responsible for the additional energy density above that provided by the relativistic particles and magnetic fields in the jets. This entrained material must have a lower temperature than the surrounding hot gas because the X-ray surface brightness decreases at the locations of the radio lobes (e.g. Croston et al. 2003). Here we consider both the case without entrained material and the case where entrained material provides five times the energy density of the relativistic electrons. The ratio of energy density between the relativistic electrons and the entrained material is not well constrained; however, a factor of 5 is typical on scales of 15–20 kpc (Croston & Hardcastle, in preparation).

We find an intergalactic gas density of $2 \pm 0.5 \times 10^{-27}$ g cm^{-3} or $2 \pm 0.5 \times 10^{-3}$ cm^{-3} when entrained thermal protons provide additional internal pressure in the jets. With the standard equipartition minimum synchrotron pressure from relativistic electrons only, the density of the intergalactic gas that NGC 4061 is travelling through is $4 \pm 1 \times 10^{-28}$ g cm^{-3} or $4 \pm 1 \times 10^{-4}$ cm^{-3}. This intergalactic gas density, for the case including entrained protons, is very similar to the density in the model fit to the X-ray-emitting intergalactic gas at the projected position of NGC 4061 (∼30 kpc from the X-ray centre). We have good reason to believe that NGC 4061 is located within the X-ray-emitting gas because the X-ray contours trace the flaring ends of the jets very closely.

5 STAR-FORMING GALAXY UGC 07049

UGC 07049 is a late-type spiral at an angular distance of 3.4 arcmin from NGC 4061. It has a radial velocity of 7551 km s^{-1} and is of the morphological type Sc. As has been mentioned earlier, this galaxy shows significant H I deficiency. Additionally, it may be travelling through the X-ray-emitting hot gas in the core of this group which makes it an interesting target in which to study how a hot IGM affects the neutral gas content of spiral galaxies.

5.1 H I content and distribution

Fig. 4 shows a high-resolution (15 × 15 arcsec^2) H I column density image of UGC 07049 overlaid on an optical *R*-band image. The H I distribution in the disc is asymmetric, with a peak in the H I south of the centre of the galaxy. A distinct feature is that the H I disc is

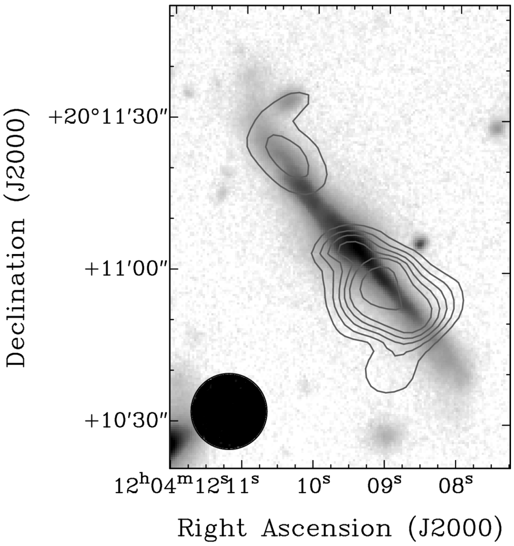

Figure 4. High-resolution (15 arcsec) total H I contours for UGC 7049 overlaid on an optical *R*-band image. The H I column density contour levels are $8.3 \times 10^{19} \times$ (3, 5, 7, 9, 11, 15, 20).

similar in extent to the optical disc. In normal late-type spirals of similar morphological type, typical H I discs are found to be 1.5–2 times larger in extent than the optical disc (Broeils & Rhee 1997). Fig. 5 shows the interferometric H I spectrum of UGC 07049 from our GMRT data. The integrated flux density as estimated from this spectrum is 0.86 Jy km s^{-1}, which matches well with the single dish value reported in Huchtmeier & Richter (1989; 0.85 Jy km s^{-1}) and is slightly lower than that reported from Arecibo observations by Springob et al. (2005; 1.12 Jy km s^{-1}). The 0.86 Jy km s^{-1} integrated flux density corresponds to an H I mass of 2×10^9 M$_\odot$. A reasonable match of the integrated line flux densities of GMRT data and single dish observations imply that we have not lost any diffuse extended emission and the H I disc is indeed similar in size as the optical disc.

The parameter that indicates whether a galaxy has lost gas compared to a field galaxy of similar size and similar morphological type is typically known as the 'H I deficiency' and is given by

$$\mathrm{def}_{\mathrm{H\,I}} = \log \frac{M_{\mathrm{H\,I}}}{D_l^2}\bigg|_{\mathrm{predicted}} - \log \frac{M_{\mathrm{H\,I}}}{D_l^2}\bigg|_{\mathrm{observed}}, \tag{3}$$

where $M_{\mathrm{H\,I}}$ is the total H I mass of a galaxy and D_l is the optical major isophotal diameter (in kpc) measured at or reduced to a surface brightness level $\mathrm{m}_B = 25.0$ mag arcsec^{-2}.

The 'predicted' field galaxy value of H I surface density for morphological type Sc has been taken from Haynes & Giovanelli (1984). While Haynes & Giovanelli (1984) used the UGC blue major diameters for D_l, in this work the major diameter is taken from the Third Reference Catalog of Bright Galaxies (RC3). To take care of the difference in the surface matter density that result from the use of RC3 diameters, a value of 0.08 (de Vaucouleurs et al. 1991) has been added to the predicted surface density given by Haynes & Giovanelli (1984). Assuming a distance of 100.7 Mpc, derived using the optical velocity of UGC 07049 and using its RC3 diameter value 0.91 arcmin, the H I deficiency of the galaxy is found to be ∼0.41. This implies that the galaxy is ∼2.6 times deficient in H I.

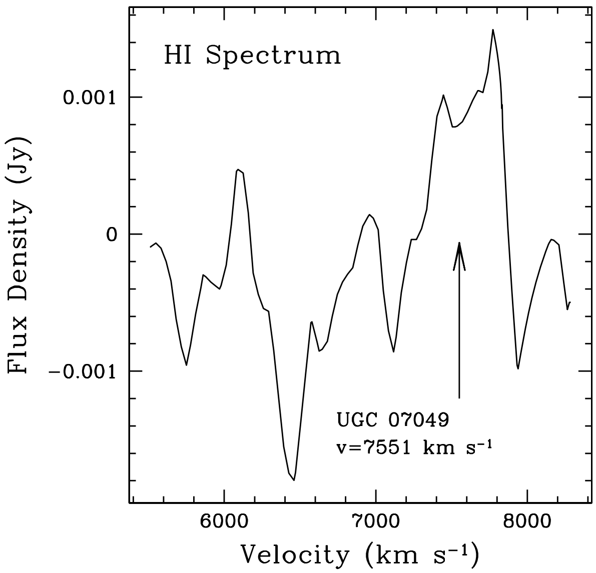

Figure 5. Interferometric H I spectrum of UGC 07049 from our GMRT data.

5.2 Ram-pressure stripping

Possible causes for the H I deficiency include tidal interactions, ram-pressure stripping, or a combination of these two processes. In the H I images we do not see any H I tidal extensions, although the stellar disc appears to be warped on the north-east end. Recent studies have shown that in groups with X-ray bright IGM ram pressure alone or tidally aided ram pressure is capable of removing a considerable fraction of the gas from constituent galaxies (Davis et al. 1997; Rasmussen, Ponman & Mulchaey 2006; Sengupta & Balasubramanyam 2006; Sengupta, Balasubramanyam & Dwarakanath 2007). The H I data presented here show the gaseous disc of UGC 07049 to be of similar size to the optical disc, whereas normal galaxies are known to have larger H I discs compared to their optical discs. Truncated H I discs are common in clusters of galaxies and in many cases are thought to result from ram-pressure stripping. The low column density gas from the outer edges of the disc is swept out by the ram pressure offered by the dense intracluster gas, leaving behind a reduced H I disc.

The NGC 4065 group has been detected to have a hot IGM and also a bent radio jet indicating resistance from the IGM. The spiral UGC 07049 is located within the projected X-ray-emitting gas. Using some simple calculations we will explore whether ram pressure in this group is strong enough to strip gas from UGC 07049. We have followed the method outlined in Sengupta et al. (2007) for calculating the possible gas loss from UGC 07049 due to ram pressure.

Ram-pressure stripping will be effective for a galaxy when the H I surface density, σ_μ, is less than $\rho_{\mathrm{IGM}} v_{\mathrm{gal}}^2/(2\pi\, G\sigma_*)$, where σ_* is the stellar surface density, ρ_{IGM} is the local IGM density and v_{gal} is the velocity with which the galaxy is moving through the medium. We use the local projected IGM density of 4×10^{-4} cm^{-3} from the X-ray gas profile, and for the velocity of UGC 07049 we consider both the 220 and 416 km s^{-1} velocity dispersion. The stellar surface density for UGC 07049 is estimated from its Two Micron All Sky Survey (2MASS) *K*-band magnitude and $K-J$ colour. Relating the mass-to-light ratio in the *K* band (M/L_K) to the $K-J$ colours (Bell & de Jong 2001) along with the relation of L_K to the absolute magnitude in *K* band (M_K) (Worthey 1994), we estimate the stellar surface density to be 0.0194 g cm^{-2}. With this value for σ_*, the critical H I surface density σ_μ beyond which ram pressure can strip gas off the galaxy is estimated to be 3.8×10^{-5} g cm^{-2} or 2.3×10^{19} cm^{-2}. We assume the H I surface density distribution inside UGC 07049 to be of constant thickness and with a Gaussian profile (Chamaraux, Balkowski & Gerard 1980),

$$\sigma(r) = \sigma_0 \, 2^{-r^2/r_{\rm H}^2}, \qquad (4)$$

where $r_{\rm H}$ is the radius within which half the H I mass is present. For σ_0 an average value of 20 M$_\odot$ pc^{-2}, as seen in normal late-type spirals (Omar & Dwarakanath 2005) in group environments was used. The central H I column density of UGC 07049 also could have been used but the disc was too disturbed and there was a central H I depletion in the high-resolution map and thus the map was not used for estimating the σ_0 value. Integrating the surface density distribution to equal the entire observed H I mass allows us to solve for $r_{\rm H}$ and find a value of 5 kpc. The radius corresponding to σ_μ is then 10 kpc (for the case where $v_{\rm gal}$ =416 km s^{-1}). Finally the H I mass outside this radius, which would be able to be ram pressure stripped, was estimated to be 7×10^7 M$_\odot$. A similar estimate of the stripped H I mass was done with the 220 km s^{-1} velocity dispersion and, understandably, produced a smaller mass-loss. These calculations assume the galaxy is travelling face-on through the IGM and they do not take into account any of the galaxy's orbital history.

Compared to the observed H I deficiency the amount of ram-pressure-stripped H I is very small, indicating that under the assumed criteria ram pressure alone would not contribute to gas loss in a significant way. However, tidal interactions have been observed to remove large amounts of H I gas from galaxies in groups (Freeland et al. 2009) and can increase the effectiveness of ram-pressure stripping. In this scenario, tidal interactions may disturb the gas disc, pull gas out and reduce the column density enabling even weak ram pressure to strip off low column density gas in large quantities. It is quite possible that UGC 07049 has undergone such stripping in this group given the richness of the system, a hostile X-ray-emitting dense IGM, lower than normal gas content, a truncated and asymmetric H I disc, and the disturbed stellar disc. In addition to these, the possibility of this galaxy to have passed through the group core and thereby experience a higher IGM density cannot be ruled out. A trip through the core of this group, experiencing intergalactic gas densities nearly 10 times higher, can ram pressure strip enough H I gas to explain the deficiency only if the galaxy velocity is as high as ~800 km s^{-1}.

5.3 Star formation rate

UGC 07049 has a 1420-MHz radio continuum flux density of 10.9 mJy (see Fig. 6). At a distance of 100.7 Mpc this corresponds to an upper limit on the star formation rate of 7 M$_\odot$ yr^{-1} using the simple relation in Yun, Reddy & Condon (2001). This assumes a Salpeter initial mass function integrated over stars with masses ranging from 0.1 to 100 M$_\odot$.

With a measured H I mass of 2×10^9 M$_\odot$ and a star formation rate of 7 M$_\odot$ yr^{-1}, UGC 07049 will exhaust its H I gas in ~300 Myr. For comparison, the crossing time for this group, assuming a diameter of 1 Mpc, is ~2 Gyr. Thus, the H I deficiency seen in UGC 07049 may also be a result of an elevated star formation rate.

6 SUMMARY

We examine two objects in the NGC 4065 group of galaxies: a bent-double radio source and an H I-deficient spiral galaxy. We use X-ray observations and the bent-double radio source to probe the density of intergalactic gas in this group. For the H I-deficient spiral, UGC 07049, we calculate the effectiveness of ram-pressure stripping as a gas-removal mechanism and find that it alone is not strong enough to produce the amount of deficiency that is observed. An elevated star formation rate is also observed in this galaxy. A combination of tidal and ram-pressure stripping, with help from the elevated star formation rate, are likely strong enough to produce the observed H I deficiency.

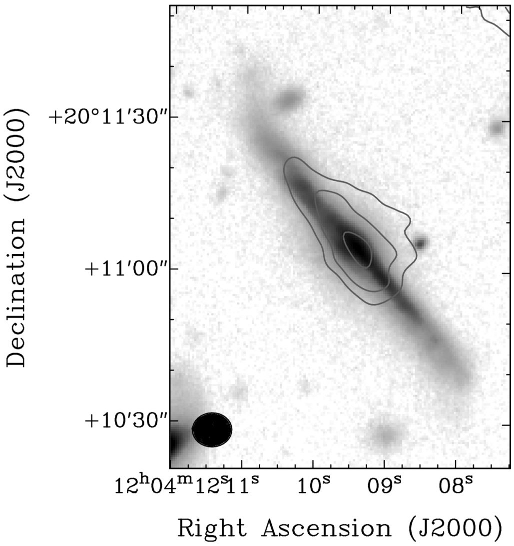

Figure 6. 20-cm radio continuum emission from UGC 07049 shown as contours on an optical *R*-band image. The lowest contour is 0.8 mJy beam^{-1} and contours increase by $\sqrt{2}$. The beam is shown in the lower left-hand corner of the image. This emission is the result of star formation in the disc of the galaxy.

ACKNOWLEDGMENTS

We thank the staff of the GMRT who have made these observations possible. GMRT is run by the National Centre for Radio Astrophysics of the Tata Institute of Fundamental Research. This research has made use of the NASA/IPAC Extragalactic Database (NED) which is operated by the Jet Propulsion Laboratory, Caltech, under contract with the National Aeronautics and Space Administration.

REFERENCES

Begelman M. C., Rees M. J., Blandford R. D., 1979, Nat, 279, 770
Bell E. F., de Jong R. S., 2001, ApJ, 550, 212
Bicknell G. V., 1984, ApJ, 286, 68
Broeils A. H., Rhee M., 1997, A&A, 324, 877
Burns J. O., Owen F. N., 1980, AJ, 85, 204
Chamaraux P., Balkowski C., Gerard E., 1980, A&A, 83, 38
Croston J. H., Hardcastle M. J., Birkinshaw M., Worrall D. M., 2003, MNRAS, 346, 1041
Croston J. H., Hardcastle M. J., Birkinshaw M., Worrall D. M., Laing R. A., 2008, MNRAS, 386, 1709
Davis D. S., Keel W. C., Mulchaey J. S., Henning P. A., 1997, AJ, 114, 613
de Vaucouleurs G., de Vaucouleurs A., Corwin H. G., Jr, Buta R. J., Paturel G., Fouque P., 1991, Third Reference Catalogue of Bright Galaxies. Springer-Verlag, Berlin
Dressler A., 1980, ApJ, 236, 351
Eke V. R. et al., 2004, MNRAS, 348, 866
Falco E. E. et al., 1999, PASP, 111, 438
Focardi P., Kelm B., 2002, A&A, 391, 35

Freeland E., Cardoso R. F., Wilcots E., 2008, ApJ, 685, 858

Freeland E., Stilp A., Wilcots E., 2009, AJ, 138, 295

Gavazzi G., O'Neil K., Boselli A., van Driel W., 2006, A&A, 449, 929

Geller M. J., Huchra J. P., 1983, ApJS, 52, 61

Girardi M., Giuricin G., Mardirossian F., Mezzetti M., Boschin W., 1998, ApJ, 505, 74

Gómez P. L. et al., 2003, ApJ, 584, 210

Goto T., Yamauchi C., Fujita Y., Okamura S., Sekiguchi M., Smail I., Bernardi M., Gomez P. L., 2003, MNRAS, 346, 601

Haynes M. P., Giovanelli R., 1984, AJ, 89, 758

Huchtmeier W. K., Richter O.-G., 1989, A General Catalog of H I Observations of Galaxies. The Reference Catalog. Springer-Verlag, Berlin

Jones T. W., Owen F. N., 1979, ApJ, 234, 818

Laing R. A., Bridle A. H., 2002, MNRAS, 336, 1161

Laing R. A., Bridle A. H., Cotton W. D., Worrall D. M., Birkinshaw M., 2008, in Rector T. A., De Young D. S., eds, ASP Conf. Ser. Vol. 386, Extragalactic Jets: Theory and Observation from Radio to Gamma Ray. Astron. Soc. Pac., San Francisco, p. 110

Lumb D. H., Warwick R. S., Page M., De Luca A., 2002, A&A, 389, 93

Mahdavi A., Geller M. J., 2004, ApJ, 607, 202

Mahdavi A., Böhringer H., Geller M. J., Ramella M., 2000, ApJ, 534, 114

O'Dea C. P., Owen F. N., 1987, ApJ, 316, 95

Omar A., Dwarakanath K. S., 2005, JA&A, 26, 34

Osmond J. P. F., Ponman T. J., 2004, MNRAS, 350, 1511

Rasmussen J., Ponman T. J., Mulchaey J. S., 2006, MNRAS, 370, 453

Sengupta C., Balasubramanyam R., 2006, MNRAS, 369, 360

Sengupta C., Balasubramanyam R., Dwarakanath K. S., 2007, MNRAS, 378, 137

Springob C. M., Haynes M. P., Giovanelli R., Kent B. R., 2005, ApJS, 160, 149

Tago E., Einasto J., Saar E., Tempel E., Einasto M., Vennik J., Müller V., 2008, A&A, 479, 927

Tully R. B., 1987, ApJ, 321, 280

Venkatesan T. C. A., Batuski D. J., Hanisch R. J., Burns J. O., 1994, ApJ, 436, 67

Worrall D. M., Birkinshaw M., 2000, ApJ, 530, 719

Worthey G., 1994, ApJS, 95, 107

Yang X., Mo H. J., van den Bosch F. C., Pasquali A., Li C., Barden M., 2007, ApJ, 671, 153

Young A., Rudnick L., Katz D., DeLaney T., Kassim N. E., Makishima K., 2005, ApJ, 626, 748

Yun M. S., Reddy N. A., Condon J. J., 2001, ApJ, 554, 803

This paper has been typeset from a TEX/LATEX file prepared by the author.